Lawrence Berkeley Laboratory
UNIVERSITY OF CALIFORNIA

Materials & Molecular Research Division

Submitted to The Journal of Chemical Physics

INHOMOGENEOUS BROADENING OF VIBRATIONAL LINEWIDTHS IN POLYATOMIC LIQUIDS

S. M. George, H. Auweter, and C. B. Harris

June 1980

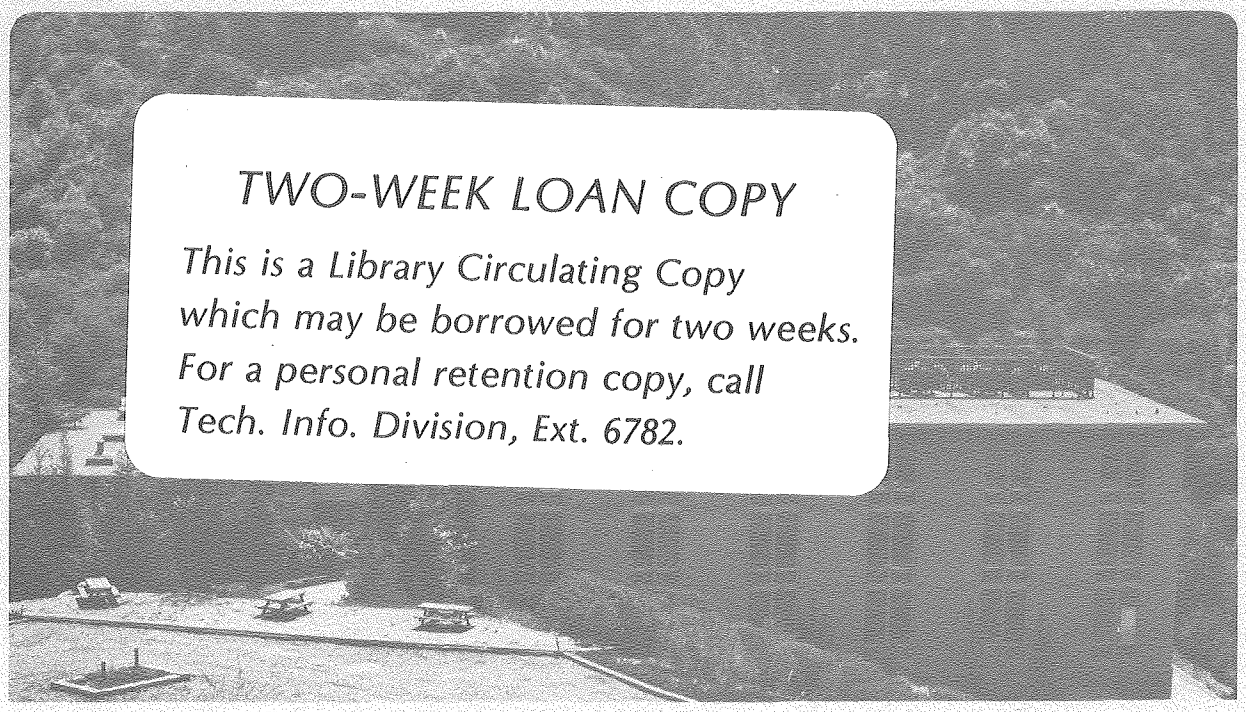

Prepared for the U.S. Department of Energy under Contract W-7405-ENG-48

DISCLAIMER

LBL#10141
Submitted to Journal of Chemical Physics

INHOMOGENEOUS BROADENING OF VIBRATIONAL LINEWIDTHS IN POLYATOMIC LIQUIDS

S. M. George, H. Auweter* and C. B. Harris

Department of Chemistry and Materials and Molecular Research Division
of Lawrence Berkeley Laboratory, University of California,
Berkeley, California 94720

*Permanent address: Physikalisches Institut, Universitat Stuttgart,
Pfaffenwaldring 57, 7000 Stuttgart-80, West Germany

ABSTRACT

The first account of inhomogeneous broadening of vibrational linewidths in non-hydrogen-bonded liquids is presented based on the combined results of isotropic spontaneous Raman studies and picosecond coherent probing experiments. The symmetric CH_3-stretching vibrational linewidths studied were found to be inhomogeneously broadened to various degrees. A correlation between the inhomogeneous broadening and the liquid's local number density distribution width is demonstrated, upon which a theoretical model for inhomogeneous broadening is developed. A stochastic lineshape theory is constructed in which homogeneous and inhomogeneous broadening are treated simultaneously in terms of one vibrational correlation function. This treatment unifies the fast and slow modulation approaches to vibrational dephasing and demonstrates how isotropic spontaneous Raman scattering studies and picosecond coherent probing experiments can be used in conjunction to study the inhomogeneous broadening of vibrational linewidths.

I. INTRODUCTION

Until recently, there has been no evidence to suggest that non-polar or non-hydrogen-bonded liquids were significantly inhomogeneously broadened and consequently most vibrational dephasing theories and studies have neither made this distinction nor addressed this possibility. In a recent paper,[1] however, we observed that even very simple non-hydrogen-bonded liquids can be significantly inhomogeneously broadened. This immediately poses an important question. Is inhomogeneous broadening in non-hydrogen-bonded liquids general, and if so, what is the physical origin of the broadening?

In order to study the inhomogeneous broadening of the symmetric CH_3-stretching liquid vibrational linewidths in a variety of liquids, isotropic spontaneous Raman scattering studies and stimulated Raman picosecond coherent probing experiments[2,3] were performed. The picosecond coherent probing experiment allows the homogeneous linewidth of a single, distinct vibrational isochromat to be determined in a vibrational lineshape which may be composed of a continuous frequency distribution of vibrational isochromats established by inhomogeneous broadening processes. Since spontaneous Raman scattering arises from all the vibrational isochromats in the distribution, isotropic spontaneous Raman scattering yields a lineshape which arises from the convolution of both the homogeneous and inhomogeneous broadening lineshape functions. Consequently, the inhomogeneous broadening lineshape function can be obtained by deconvoluting the homogeneous lineshape function determined by the picosecond experiment from the isotropic spontaneous Raman lineshape function. Thus the inhomogeneous broadening of vibrational lineshapes in liquids can be studied and related to structural and/or dynamic properties of the liquid.

In this paper we would like to establish the generality of inhomogeneous broadening of symmetric CH_3-stretching vibrations in non-hydrogen-bonded polyatomic liquids and to suggest a simple model for the broadening's magnitude which is based on the width of the distribution of the liquid's local number densities. Moreover, we would like to develop a stochastic lineshape theory which treats homogeneous and inhomogeneous broadening simultaneously in terms of one vibrational correlation function and demonstrate how isotropic spontaneous Raman scattering studies and picosecond coherent probing experiments can be used to study the inhomogeneous broadening of vibrational linewidths.

II. EXPERIMENTAL

The stimulated Raman scattering experiments were performed with single picosecond pulses selected from the rising edge of pulse trains emitted from a stabilized, passively-modelocked Nd:glass laser.[4] After amplification, compression, and frequency-doubling the pulses had a duration of $\cong$ 5 psec and a spectral bandwidth (FWHM) of $\cong$ 4 cm^{-1}, yielding a bandwidth product of $\cong$ 0.6, which indicates that the pulses were essentially bandwidth-limited. The pulses were compressed by passage through a 1 cm cell of Eastman Kodak dye #9860 with OD = 3.0 at 10,600 A. The dye effectively absorbs the rising edge of the pulse, then bleaches, allowing the main portion of the pulse to pass. This establishes a very rapid rising edge of $\lesssim$ 0.7 psec on the pulse but does not significantly broaden the pulse's spectral bandwidth. The compressed pulse was broadened by $\lesssim$ 6% relative to an uncompressed pulse.

Each pulse was split into an excitation pulse and a delayed probe pulse. The polarization of the probe pulse was rotated such that the probe pulse was polarized perpendicularly with respect to the excitation pulse. The excitation and probe pulses were recombined collinearly in a 10 cm sample cell.

The symmetric CH_3-stretching vibrations were coherently excited by transient stimulated Raman scattering.[5] Coherent excitation establishes a macroscopic coherent superposition of vibrational states v=0 and v=1 in a group of symmetric CH_3-stretching vibrations, i.e. $\rho_{01}(t)$, an off-diagonal

density matrix element in the symmetric CH_3-stretching vibrational oscillator basis set. The excitation process is highly non-linear and model calculations have demonstrated an abrupt onset and cutoff of the pumping process due to the sharp rise and decay of the stimulated Stokes pulse.[3,5]

The coherently excited symmetric CH_3-stretching vibrations were probed by coherent strokes Raman scattering. The macroscopic coherent superposition of vibrational states v=0 and v=1 oscillates with a well-defined phase and produces a macroscopic modulation of the optical refractive index at the vibrational frequency through the coupling parameter $\delta\alpha/\delta q$, the change of polarizability, α, with vibrational coordinate, q. The incoming probe pulse scatters off this modulated refractive index, producing sidebands, i.e. beat frequencies shifted by the vibrational frequency to higher and lower frequencies. The efficiency of coherent scattering is crucially dependent on the spatial wave vector k-matching condition defined by the probe scattering geometry.[3] For selective k-vector matching in a 10 cm sample cell, the coherent Stokes probe scattering is derived only from vibrations located within a frequency interval of $\simeq$ 0.3 cm^{-1} around the center of the spontaneous vibrational line.[2,3] Thus the Stokes probing technique can detect a homogeneously broadened vibrational isochromat as narrow as 0.3 cm^{-1} in a vibrational linewidth of unknown inhomogeneity. This sets an upper limit of $T_2/2 \leq 18$ psec on the decay time resolution . Assuming an impulse excitation, the lower limit on the decay time resolution in an excite and probe experiment is established by the rising edge of the probe laser pulse. Since the pulses have a sharp rising edge of $\leq$ 0.7 psec, $T_2/2$ decay times longer than 0.7 psec can be resolved.[6]

The coherently scattered Stokes probe signal and the excitation Stokes spectrum were separated and *simultaneously* detected on the target of a two-dimensional optical multichannel analyzer. We used pulses near the threshold for stimulated Raman scattering, spectrally observed each shot and discarded any shot that displayed frequency modulation. The experimental setup for stimulated Stokes excitation and coherent Stokes probe scattering is depicted schematically in Figure 1.

The coherently scattered Stokes signal decays exponentially with a slope of $T_2/2$ as a function of probe pulse delay.[2,3,7] Since the signal decays exponentially, the vibrational dephasing time, T_2, is proportional to the inverse of the linewidth of the homogeneous Lorentzian lineshape function:

$$\Delta w \text{ (FWHM) } cm^{-1} = \frac{1}{c\pi T_2} \qquad (1)$$

Thus the linewidth of the homogeneous Lorentzian lineshape can be determined by measuring T_2, the homogeneous vibrational dephasing time.

Isotropic spontaneous Raman lineshapes were obtained using a standard Argon ion laser and a double monochromator scattering unit. The polarized Stokes scattering lineshapes were essentially the same as the isotropic lineshapes because of the very small depolarization factor for the symmetric CH_3-stretching vibrations in the liquids studied.

III. RESULTS

Figure 2 shows the coherently scattered Stokes signal as a function of probe pulse delay for the symmetric CH_3-stretching vibration in methanol and ethanol. On the average, the observed dephasing times were $T_2/2 = 1.2 \pm 0.5$ psec for methanol[1] and 1.25 ± 0.5 psec for ethanol.[8,9] The isotropic Raman lineshapes of the same vibrations are also shown in Fig. 2. From the measured dephasing times, we calculate the corresponding homogeneous Lorentzian lineshapes which are also drawn in Fig. 2. From these superimposed lineshapes the inhomogeneous broadening in these two hydrogen-bonded liquids can easily be visualized.

Figure 3 shows the coherently scattered Stokes signal as a function of probe pulse delay for the symmetric CH_3-stretching vibration in acetone and methyl sulfide. On the average, the observed dephasing times were $T_2/2 = 1.5 \pm 0.5$ psec for acetone and 1.9 ± 0.5 psec for methyl sulfide. The isotropic Raman lineshapes and homogeneous Lorentzian lineshapes corresponding to the measured dephasing times are also shown in Fig. 3. The superimposed lineshapes display significant inhomogeneous broadening for both of these non-hydrogen-bonded liquids. Two more examples of non-hydrogen-bonded liquids are given in Figure 4 for trichloroethane and acetonitrile. There was no observable broadening within the error limits in trichloroethane, which is consistent with the results of Laubereau et al.[10,11,12]

The average experimental dephasing times, calculated homogeneous linewidths, and isotropic Raman linewidths for all the liquids studied are compiled in Table 1. We found that *symmetric CH_3-stretching vibrational linewidths in non-hydrogen-bonded liquids are inhomogeneously broadened to various degrees.*[13]

Thus the symmetric CH_3-stretching vibrational linewidths of non-hydrogen-bonded liquids are not motionally narrowed, presumably because the liquid site relaxation times are much longer than earlier predictions.

IV. INHOMOGENEOUSLY BROADENED LINESHAPE ANALYSIS

If the liquid vibrational band is inhomogeneously broadened, the lineshape observed by isotropic spontaneous Raman scattering arises from the convolution of two independent lineshape functions: L(w), the homogeneous lineshape function which is Lorentzian; and G(w), the inhomogeneous broadening lineshape function. The resultant vibrational lineshape function, I(w), can be written as a convolution integral:

$$I(w) = \int_{-\infty}^{\infty} L(w')G(w-w')dw' \qquad (2)$$

Since isotropic spontaneous Raman scattering gives the lineshape for I(w) and the picosecond measurement gives the homogeneous Lorentzian lineshape, L(w), the inhomogeneous broadening lineshape, G(w), can be obtained by deconvoluting the isotropic spontaneous Raman and homogeneous Lorentzian lineshapes. Unfortunately, I(w) is not easily represented by a simple functional form. In most cases, however, I(w), the isotropic spontaneous Raman scattering lineshape, is somewhere in between a Gaussian and Lorentzian lineshape.

One well-studied lineshape which is intermediate between a Gaussian and a Lorentzian is a Voigt profile, which is a convolution of independent Gaussian and Lorentzian lineshapes.[14,15] If the isotropic spontaneous Raman lineshape is assumed to be a Voigt profile, which is usually the case, and the inhomogeneous broadening lineshape is assumed to be a Gaussian,[16] the problem of deconvolution is greatly simplified. Numerical deconvolution is not necessary because if the linewidths for the Voigt and Lorentzian lineshapes are known, the linewidth for the Gaussian lineshape can be determined from numerical Voigt profile tables.[15] The linewidths for G(w), the inhomogeneous broadening lineshape function, were determined after making the above assumptions and are listed in Table 1.

Several general observations can be made about the data in Table 1. First, the homogeneous widths are rather uniform relative to the inhomogeneous widths. Second, even non-polar liquids such as pentane are highly inhomogeneously broadened. Moreover, although the hydrogen-bonded liquids display the greatest inhomogeneous broadening, they do not form a class by themselves. Several non-hydrogen-bonded liquids are broadened almost as much as the hydrogen-bonded liquids.

V. DISCUSSION

After determining that the inhomogeneous broadening lineshape linewidths varied from 1 to 15 cm^{-1}, attempts were made to correlate the inhomogeneous broadening linewidths with various liquid parameters. Initially, we assumed that the inhomogeneous broadening was determined by a distribution of environmental sites which establishes a certain continuous frequency distribution of vibrational isochromats. This assumption is supported by studies on hydrogen-bonded liquids[17,18] which suggest that the *attractive* portion of the intermolecular potential, viz. the hydrogen bond, causes long range correlations in the intermolecular forces and creates a distribution of environmental sites which establishes a distribution of vibrational frequencies. Furthermore, recent picosecond experiments have demonstrated that hydrogen-bonded liquids are severely inhomogeneously broadened,[2]

presumably because the attractive portion of the intermolecular potential causes long-range correlations which enable environmental sites to persist for $\geq$ 5 psec. Since the attractive portion of the intermolecular potential is implicated in the inhomogeneous broadening of hydrogen-bonded liquids, attempts were made to correlate the inhomogeneous broadening in the non-hydrogen-bonded liquids with various liquid intermolecular attraction

parameters. No correlation was observed, however, with: Trouton's ratio; B.P./M.W. (Boiling Point/Molecular Weight); μ, the molecular dipole moment; the hydrogen bonding parameter; or α, the polarizability. In addition, no correlation was observed with the Kirkwood dipole correlation factor.[19,20] Some of the attempted correlations are shown in Figures 5-8 and the liquid parameter values are listed in Table 2.

The ultrasonic absorption constant, α/α_{class}, the ratio of the observed ultrasonic absorption constant and the predicted classical ultrasonic absorption constant, is related to liquid structural associativity.[21,22] The ultrasonic absorption constant displayed a slight correlation with the inhomogeneous broadening which is shown in Figure 9. Trichloroethane and methyl iodide, two linewidths which are broadened the least, have the largest ultrasonic absorption constant. This behavior is consistent with Pinkerton's liquid classification scheme, which groups liquids with large ultrasonic absorption constants into the non-associated liquid division.[21] The other liquids, which are more severely broadened, have ultrasonic absorption constants which are closer to the associated liquid division of the Pinkerton classification scheme. This correlation requires further investigation. Parameters used to calculate α/α_{class}, the ultrasonic absorption constant, are listed in Table 3.

Since the inhomogeneous broadening lineshape linewidths did not correlate with liquid attraction parameters, attempts were made to find a correlation with other liquid parameters. The inhomogeneous broadening does tend to scale with the molecule's deviation from spherical symmetry. The simplest, most spherical molecules, trichloroethane and methyl iodide, are nearly homogeneous, whereas the longest, least spherical molecules, methyl formate and pentane are extremely inhomogeneous. This suggests that the

molecule's shape determines how the molecule can pack with other molecules, which may influence the number of environmental sites that are formed in the liquid.[23]

In addition, a correlation was observed between the inhomogeneous broadening linewidth and the liquid's free volume.[24] The correlation is shown in Figure 10 and the parameters used to calculate the liquid's free volume are listed in Table 4. This correlation suggests that the liquid's entropy participates in establishing the number of environmental sites in the liquid since the liquid's entropy may cause the liquid's free volume to distribute itself in order to maximize the number of interactions of molecules with other molecules and/or free space. In such a case, the number of different environmental sites in the liquid would be functionally dependent upon the liquid's free volume.

Free volume alone does not elucidate the *distribution* of values in a local liquid parameter which may give rise to a *distribution* of environmental sites. The liquid's free volume, however, is closely related to the distribution width of the liquid's local number density through the isothermal compressibility. Since a distribution of local number densities could conceivably create a distribution of distinct vibrational frequencies, this parameter will be derived and discussed in detail.

Following the standard treatment,[25,26] we treat the liquid as an open, isothermal system of volume V, and apply the method of most probable distributions to characterize the spread in the distribution of the number of molecules, N,

$$\bar{N}^2 - (\bar{N})^2 = \sigma_N^2 = kT\left(\frac{\partial \bar{N}}{\partial \mu}\right)_{V,T} \qquad (3)$$

where μ is the chemical potential. Introducing the number density, $\rho = \frac{N}{V}$,

and using the relation $d\mu = Vdp$, one can show that:

$$\sigma_N^2 = (\bar{N})^2 \, kT \, \frac{K_T}{V} \tag{4}$$

where K_T is the isothermal compressibility of the liquid. Since V is constant, equation (4) can be rewritten to yield σ_ρ, the fluctuation in the liquid's number density:

$$\sigma_\rho = \bar{\rho} \sqrt{\frac{kT \, K_T}{V}} \tag{5}$$

σ_ρ characterizes the spread in the number density distribution, i.e. the root mean-square deviation from the mean of the number density. We will refer to σ_ρ as the *local* number density distribution width since the volume, V, can be arbitrarily scaled down to molecular dimensions.

In order to calculate σ_ρ, the local number density distribution width, values for the isothermal compressibility are needed. Unfortunately, very few experimental liquid isothermal compressibility values have been determined. The isothermal compressibility, K_T, can be calculated, however, using the equation:[27]

$$K_T = \left[\frac{1}{K_o} - \frac{2}{V} \left(\Delta H_{vap} - RT\right)\right]^{-1} \tag{8}$$

where K_o is the isothermal compressibility for a fluid of hard spheres:

$$K_o = \left(\frac{V}{NkT}\right) \left[\frac{(1+y)^2}{(1+2y)}\right]^2 \tag{7}$$

This equation is derived from the free volume theory of liquid and has been shown to give satisfactory agreement with experimental values.[27] In the

expression for K_o, the packing fraction of the liquid, y, is defined as:

$$y = \frac{\pi}{6} \rho_l \sigma^3 \tag{8}$$

where ρ_l is the number density of the liquid and σ is the hard sphere diameter. The hard sphere diameter can be approximated using the relationship:[28]

$$\sigma^3 = \frac{1.04}{\rho_s} \tag{9}$$

where ρ_s is the number density of the solid at the melting point.[29] All parameter values, calculated isothermal compressibilities and local number density distribution widths are listed in Table 5.

Figure 11 shows a graph of the inhomogeneous broadened linewidth magnitudes versus $\sigma_\rho \propto \bar{\rho}\sqrt{K_T}$. This plot demonstrates that *the amount of inhomogeneous broadening is approximately proportional to the liquid's local number density distribution width.* This correlation suggests that either the local number density distribution causes the inhomogeneous broadening, or that the local number density distribution width scales with some other liquid property that causes the inhomogeneous broadening.

VI. STOCHASTIC LINESHAPE THEORY FOR INHOMOGENEOUS BROADENING

In order to develop a model for inhomogeneous broadening of vibrational transitions in a more formal way, the inhomogeneous broadening problem was constructed in the time-domain. The Kubo-Anderson general stochastic theory of lineshape[30,31a] provides a simple theoretical framework from which inhomogeneous broadening can be formalized and visualized. Formally, the Hamiltonian for the vibrational oscillators can be written:

$$H = H_o + H_p + H_m \tag{10}$$

where

$$H_o = \sum_j \hbar(w_o + \Delta w(t)) a_j^+ a_j \tag{11}$$

$$H_p = \sum_j n_j V(a_j, a_j^+, R_j(r), \theta_j(r)) \tag{12}$$

$$H_m = \sum_{j,k} \hbar g_{jk} (a_j a_k^+ + a_k a_j^+) \tag{13}$$

$$g_{jk} = F(R_j(r,t), R_k(r,t), \theta_j(r,t), \theta_k(r,t)) \tag{14}$$

The subscript j sums over the various environmental sites and n_j is the population fraction at each site. H_o is the unperturbed Hamiltonian containing $\Delta w(t)$, which gives rise to the homogeneous lineshape of each vibrational isochromat. H_p is the perturbing Hamiltonian which causes a frequency splitting according to the particular environmental sites which are dependent upon $R_j(r)$, the molecular radial distribution around site j and $\theta_j(r)$, the molecular orientation factor around site j. H_m is the motional Hamiltonian which interconverts environmental sites at a rate, g_{jk}, determined by changes in the molecular distribution and orientation.

The commutation relationships are as follows:

$$[H_o, H_m] \approx 0 \tag{15}$$

$$[H_o, H_p] \neq 0 \tag{16}$$

$$[H_m, H_p] \neq 0 \tag{17}$$

H_o commutes with H_m in the limit that H_o and H_m operate on different timescales. Since $\Delta w(t)$, viz. the time-dependent processes in H_o which give

rise to the homogeneous linewidth, occurs on the picosecond or subpicosecond timescale and g_{jk}, the site interconversion rate, occurs on the timescale of diffusion or rotation, this limit is probably obeyed.

H_p does not commute with H_o, therefore H_p can change w_o, the natural frequency of H_o. H_m does not commute with H_p, therefore H_m causes a time variation of H_p according to:

$$i\hbar \dot{H}_p = [H, H_p] \tag{18}$$

$$= [H_o, H_p] + [H_m, H_p] \tag{19}$$

$[H_o, H_p] \approx 0$ since H_p is assumed to have no important matrix elements connecting various unperturbed states of H_o. H_p only changes the frequency without causing transitions.

These are the formal Hamiltonians and their precise form is not known. In the absence of exact Hamiltonians, however, a randomly modulated oscillator model can be used.[31] This approach treats the vibration as an oscillator with a randomly modulated frequency and allows *both* the homogeneous and inhomogeneous broadening problems to be treated easily.

In this treatment, the vibrational oscillator, with a natural frequency w_0, is given an equation of motion:

$$\dot{x} = iw(t)x \tag{20}$$

where w(t) is the frequency with random modulation. The time average of w(t) is w_0 and w(t) can be written as:

$$w(t) = w_0 + w_1(t) \tag{21}$$

where $w_1(t)$, the stochastic process, represents the fluctuation in frequency.

$w_1(t)$ can be described in terms of two characteristic parameters: Δ, the amplitude of the frequency change during the modulation; and τ_c, the correlation time of the modulation. Given a probability distribution $P(w_1)$ for the frequency modulation:

$$\Delta^2 = \int w_1^2 P(w_1) dw_1 \tag{22}$$

and

$$\tau_c = \int_o^\infty \psi(\tau) d\tau \tag{23}$$

where

$$\psi(\tau) = \frac{1}{\Delta^2} \langle w_1(t) w_1(t+\tau) \rangle \tag{24}$$

A relaxation function, $\phi(t)$, can be defined for the oscillator.

$$\phi(t) = \langle \exp i \int_o^t w_1(t') dt' \rangle \tag{25}$$

If $w_1(t)$, the frequency displacement modulation, is a Guassian process:

$$\phi(t) = \exp[-\Delta^2 \int_o^t (t-\tau)\psi(\tau) d\tau] \tag{26}$$

If $\psi(\tau)$, the correlation function for the modulation, is assumed to be exponential, i.e. $\psi(\tau) = \exp[-t/\tau_c]$, the relaxation function, i.e. the correlation function, of the oscillator can be written:[32]

$$\phi(t) = \exp\{-\Delta^2 [\tau_c^2 (\exp(-t/\tau_c) - 1) + t\tau_c]\} \tag{27}$$

If the liquid has slowly varying intermolecular forces creating local structure, individual vibrational oscillators can vibrate in a distribution of different molecular environments which establishes a frequency distribution of vibrational isochromats. The frequency distribution of vibrational isochromats causes vibrational dephasing because of destructive interference among the

individual frequencies in the distribution. The slowly varying intermolecular forces can be characterized by a frequency modulation amplitude, $\Delta_{INH} = \sum_j n_j \Delta_j$, which can be formally derived from H_p, and a modulation correlation time, τ_{INH}, which is related to the time dependence of H_p, through in $\dot{H}_p = [H_m, H_p]$. These characteristics define the vibrational correlation function contributed by the slowly varying intermolecular forces:

$$\phi(t)_{INH} = \exp\{-\Delta^2_{INH}[\tau^2_{INH}(\exp(-t/\tau_{INH}) - 1) + t\tau_{INH}]\} \tag{28}$$

In addition to the slowly-varying intermolecular forces, short-range, rapidly varying dynamical modulation processes can cause vibrational dephasing of individual vibrational subunits. The short-range, rapidly varying modulation processes can be characterized by a frequency modulation Δ_H and a modulation correlation time τ_H. These quantities can be derived from $\Delta w(t)$ in H_o. Particular forms for $\Delta w(t)$ are given by the binary collision model,[33] the exchange theory model,[34] the hydrodynamic model,[35a] molecular dynamics simulations,[35b] the cell model,[35c] and other various models which treat a harmonic oscillator coupled to a heat bath.[7, 35d, 35e, 35f] The characteristics of the rapid, short-range modulation processes define the vibrational correlation function for an individual vibrational isochromat:

$$\phi(t)_H = \exp\{-\Delta^2_H[\tau_H{}^2(\exp(-t/\tau_H) - 1) + t\tau_H]\} \tag{29}$$

$[\Delta^2_H \tau_H]^{-1}$ in the above expression is equivalent to T_2, the homogeneous

vibrational dephasing time, for $t \geq \tau_H$ in the limit of fast modulation.[32]

Since the homogeneous vibrational linewidth, i.e. the linewidth for individual vibrational isochromat, comprises a substantial fraction of the spontaneous Raman lineshape, the spontaneous Raman lineshape is treated as a convolution of two independent lineshapes. Likewise, the vibrational correlation function corresponding to the spontaneous Raman inhomogeneous broadened lineshape must be *expressed as a product of two modulation correlation functions.* The product is strictly valid only when $\phi_H(t)$ and $\phi_{INH}(t)$ decay on different timescales. This is tantamount to the requirement that H_o and H_m must operate on different timescales in order for them to commute.

$$\phi(t) = \phi(t)_H \, \phi(t)_{INH} \tag{30}$$

The vibrational spectrum is related to the vibrational correlation function by:

$$I(w) = \frac{1}{2\pi} \int_{-\infty}^{\infty} \exp[-iwt]\phi(t)dt \tag{31}$$

Because $I(w) = \int_{-\infty}^{\infty} L(w')G(w-w')dw'$ for inhomogeneous broadened spontaneous Raman lineshapes:

$$\int_{-\infty}^{\infty} L(w')G(w-w')dw' = \frac{1}{2\pi} \int_{-\infty}^{\infty} \exp[-iwt]\phi(t)dt \tag{32}$$

$$= \frac{1}{2\pi} \int_{-\infty}^{\infty} \exp[-iwt]\phi(t)_H \phi(t)_{INH} dt \tag{33}$$

Since the Fourier transform of a product of two functions is given by the convolution integral over the products of Fourier transforms of the separate factors, $L(w)$ can be identified as the Fourier transform of $\phi(t)_H$ and $G(w)$ can be identified as the Fourier transform of $\phi(t)_{INH}$. Thus

the problem of inhomogeneous broadening has been constructed in the time-domain. This is useful because the time domain picture easily relates the inhomogeneous and homogeneous broadening to frequency displacement amplitudes and correlation times, and treats the inhomogeneous and homogeneous broadening *simultaneously* in terms of one vibrational correlation function.

This stochastic lineshape theory unifies the various slow and fast modulation approaches to vibrational dephasing. In the slow modulation limit, represented by the static environment theory of Bratos et al.[36a, 36b], a static frequency distribution of vibrational isochromats causes vibrational dephasing because of destructive interference among the individual frequencies in the distribution. In the fast or intermediate-modulation limit, represented by the theories of Fischer and Laubereau,[33] Harris et al.,[34] Oxtoby[35a, 35b], and others,[7, 35c, 35d, 35e, 35f] rapidly varying processes cause vibrational dephasing by randomly modulating the frequency of the individual vibrational isochromats. These various slow and fast modulation theories of vibrational dephasing can be unified by using the parameters τ_H, τ_{INH}, Δ_H and Δ_{INH} to define the vibrational correlation function.

The amount of inhomogeneous broadening was previously demonstrated to be approximately proportional to the liquid's local number density distribution width. Now a model is developed which relates the local number density distribution width to Δ_{INH} and τ_{INH}. First, we propose that Δ_{INH} *is related to the mean intermolecular force that the environment imposes on a molecular vibration.* Second, we propose that the *intermolecular force has a distribution which is proportional to the local number density distribution.* Therefore:

$$\Delta_{INH} \alpha \sigma_p \tag{34}$$

Δ_{INH} can be formally derived from $H_p = \sum_j n_j V(a_j, a_j^+, R_j(r), \theta_j(r))$ or $\Delta_{INH} = \sum_j n_j \Delta_j$ where individual Δ_j values result from the particular $R_j(r)$ and $\theta_j(r)$ configurations which give rise to the site. Specific local number densities in the local number density distribution affect Δ_j through $R_j(r)$ and possibly $\theta_j(r)$.

Third, we expect that τ_{INH}, the inhomogeneous broadening modulation correlation time, *is proportional to the time required for positional or orientational interconversion of molecules*, i.e. proportional to diffusion or rotation times. This can be derived from $i\hbar \dot{H}_p = [H_m, H_p]$. Since $H_p = \sum_j n_j V(a_j, a_j^+, R_j(r), \theta_j(r)$ and $H_m \alpha F(R_j(r,t), \theta_j(r,t))$, the changes in $R_j(r,t)$ and $\theta_j(r,t)$ give rise to a time variation in H_ρ. Formally, H_m is constructed as an exchange Hamiltonian. In time τ_{INH}, therefore, site j is converted to some site k because of positional, $R_j(r,t)$, and orientational, $\theta_j(r,t)$, movements of molecules.

We anticipate that τ_{INH} for the larger, elongated molecules (e.g. pentane, acetic anhydride) will have the same timescale as diffusion since their rotational movements are severely restricted. The smaller, nearly spherical molecules (e.g. trichloroethane, methyl iodide) may have τ_{INH} faster than their diffusion times because of rapid orientational averaging of $\theta_j(r,t)$ due to rotational movement.

In the limit that $\Delta_{INH}\tau_{INH} << 1$, the application of the above theory predicts that the vibrational lineshape should be a homogeneously broadened Lorentzian.[31] The Lorentzian lineshape observed for trichloroethane, which is known to be homogeneous because of the picosecond data, correctly obeys this limit. Furthermore, because Δ_{INH} is low since $\Delta_{INH} \alpha \sigma_\rho$ and τ_{INH} is short since the molecule is nearly spherical, $\Delta_{INH}\tau_{INH}$ for trichloroethane qualitatively agrees with the limit $\Delta_{INH}\tau_{INH} << 1$.

In the limit that $\Delta_{INH}\tau_{INH} >> 1$, the theory predicts that the vibrational lineshape should be an inhomogeneously broadened Voigt profile.[31] The Voigt profile lineshape for acetone, which is known to be inhomogeneously broadened because of the picosecond data, correctly obeys this limit. Moreover, because Δ_{INH} is large since $\Delta_{INH} \alpha \sigma_\rho$ and τ_{INH} is longer since the molecule is elongated, $\Delta_{INH}\tau_{INH}$ for acetone qualitatively agrees with the limit $\Delta_{INH}\tau_{INH} >> 1$.

Finally, we observed that $\Delta\omega_{INH}$, the linewidth of the inhomogeneous broadening lineshape function is approximately proportional to σ_ρ, the local number density distribution width. In addition, the broadening must be proportional to $f(\tau_{INH})$, a function dependent upon τ_{INH}, the inhomogeneous broadening correlation time. Therefore we propose that *the linewidth of the inhomogeneous broadening lineshape function is proportional to the product*

of σ_ρ (or Δ_{INH}) and $f(\tau_{INH})$:

$$\Delta\omega_{INH} \alpha f(\tau_{INH})\sigma_\rho \tag{35}$$

In the limit $\tau_{INH} \rightarrow 0$, i.e. the fast modulation limit $\Delta_{INH}\tau_{INH} << 1$, the lineshape is Lorentzian and $f(\tau_{INH})$ approaches $\Delta_{INH}\tau_{INH}/\pi c$ in order to give the correct linewidth for a Lorentzian lineshape:

$$\Delta\omega_{INH}(FWHM)\ cm^{-1} = \left(\frac{\Delta_{INH}\tau_{INH}}{\pi c}\right)\Delta_{INH} \tag{36}$$

$$= \frac{\Delta^2_{INH}\tau_{INH}}{\pi c} \tag{37}$$

$$\alpha \frac{\sigma_\rho^2 \tau_{INH}}{\pi c} \tag{38}$$

In this limit, the inhomogeneous broadening processes have become homogeneous processes.

In the limit $\tau_{INH} \rightarrow \infty$, i.e. the static environment limit developed by Bratos et al.,[36] the inhomogeneous broadening lineshape function is Gaussian and $f(\tau_{INH})$ approaches the factor $(2\ell n2)^{\frac{1}{2}}/\pi c$ in order to give the correct linewidth for a Gaussian lineshape:

$$\Delta\omega_{INH}(FWHM)\ cm^{-1} = \frac{(2\ell n2)^{\frac{1}{2}}}{\pi c}\Delta_{INH} \tag{39}$$

$$\alpha \frac{(2\ell n2)^{\frac{1}{2}}}{\pi c}\sigma_\rho \tag{40}$$

The picosecond data is in the best agreement with this limit since $\Delta\omega_{INH}$ is approximately proportional to σ_ρ.

VII. SUMMARY

We believe this is the first account of inhomogeneous broadening in non-hydrogen-bonded liquids and the first attempt to relate inhomogeneous broadening to various liquid parameters. We emphasize that symmetric CH_3-stretching vibrational linewidths in non-hydrogen-bonded liquids are inhomogeneously broadened to various degrees. A correlation is established between the inhomogeneous broadening and the liquid's local number density distribution width upon which a model for inhomogeneous broadening is constructed. A stochastic lineshape theory is developed in which homogeneous and inhomogeneous broadening processes are treated simultaneously in terms of one vibrational correlation function. This treatment unifies the fast and slow modulation approaches to vibrational dephasing and demonstrates how isotropic Raman scattering studies and picosecond coherent probing experiments can be used in conjunction to study the inhomogeneous broadening of vibrational linewidths. Since this study focused only on symmetric CH_3-stretching vibrations, additional investigations on other vibrational modes are necessary in order to demonstrate the generality of these results. Further studies to verify the correlation of inhomogeneous broadening with the liquid's number density distribution width and to explore the mechanism of inhomogeneous broadening of liquid vibrational linewidths are currently in progress.

VIII. ACKNOWLEDGEMENTS

This work was supported in part by the National Science Foundation and by the Division of Chemical Sciences, Office of Basic Energy Sciences U. S. Department of Energy, under Contract No. W-7405-Eng-48. H. Auweter gratefully acknowledges support from the Deutsche Forschungsgemeinschaft for a postdoctoral fellowship. The authors would like to thank Bostick U. Curry for his help on the isotropic Raman lineshapes. We are also appreciative to Lawrence R. Pratt for many useful discussions.

1. C. B. Harris, H. Auweter and S. M. George, Phys. Rev. Lett. 44, 737 (1980).

2. A. Laubereau, G. Wochner and W. Kaiser, Chem. Physics 28, 363 (1978).

3. A. Laubereau and W. Kaiser, Rev. Mod. Phys. 50, 607 (1978).

4. The laser system will be described in detail elsewhere.

5. R. L. Carman, F. Shimizu, C. S. Wang and N. Bloembergen, Phys. Rev. A2, 60 (1970).

6. Calculations based on the theory of the coherent Raman probing process demonstrate that T_2 (dephasing) times in which t_L (laser pulse width) > T_2 are observable (Ref. 3). For example, using 5 psec Gaussian pulses, these studies have shown that exponential decay due to dephasing begins a factor of 3 below the signal maximum for T_2 = 5 psec and a factor of 20 below the signal maximum for T_2 = 1.3 psec. These calculations illustrate the importance of observing the dephasing decay over many orders of magnitude. In comparison to a Gaussian pulse, the resolution is considerably better for a pulse with a sharp rising edge.

7. D. W. Oxtoby, Advan. Chem. Phys. 40, 1 (1979).

8. This time is much longer than the dephasing time, T_2 = 0.52 psec, for ethanol reported earlier by von der Linde et al. using a coherent Anti-Stokes scattering geometry (Ref. 9). The shorter decay time was observed because the coherent Anti-Stokes geometry is *non-selective* and therefore observes the decay of a *distribution* of vibrational subunits, which effectively dephases because of interference between the distinct frequencies of the subunits. All vibrational dephasing times determined using the coherent Anti-Stokes geometry are doubtful if the vibrational bands studied are inhomogeneously broadened.

9. D. von der Linde, A. Laubereau and W. Kaiser, Phys. Rev. Lett. 26, 954 (1971).

10. A. Laubereau, D. von der Linde and W. Kaiser, Phys. Rev. Lett. 28, 1162 (1972).

11. S. F. Fischer and A. Laubereau, Chem. Phys. Lett. 55, 189 (1978).

12. This dephasing time is in agreement with the dephasing times T_2 = 2.4 and 2.6 psec, reported by Laubereau et al. using both coherent Anti-Stokes and coherent Stokes scattering geometries (Ref. 10, 11). The linewidth in trichloroethane is almost entirely *homogeneously* broadened, so both geometries should yield the same result.

13. Our results seriously jeopardize some of the conclusions of isotropic spontaneous Raman lineshape investigations, which assumed that vibrational linewidths were homogeneous in order to extract dynamical information. Unless the vibrational linewidth is known to be homogeneous under all experimental conditions, isotropic spontaneous Raman lineshape investigations can say nothing definitive about the homogeneous linewidth.

14. B. DiBartola, *Optical Interactions in Solids* (John Wiley, New York, 1968), p. 357 ff.

15. J. T. Davies and J. M. Vaughan, The Astrophysical Journal 137, 1302 (1963).

16. A Gaussian lineshape is consistent with the theory of stochastic processes when modulation correlation times are long so that $\Delta\tau_c >> 1$, i.e. the slow modulation limit (Ref. 31).

17. G. C. Pimentel and A. L. McClellan, *The Hydrogen Bond* (Freeman, San Francisco, 1960).

18. M. V. Thiel, E. D. Becker and G. C. Pimentel, J. Chem. Phys. 27, 95 (1957).

19. Y. Marcus, *Intro. to Liquid State Chemistry* (John Wiley, New York, 1977), p. 108.

20. R. H. Cole, J. Chem. Phys. 27, 33 (1957).

21. J. M. M. Pinkerton, Proc. Phys. Soc. (London) 662, 129 (1949).

22. K. F. Herzfeld and T. A. Litovitz, *Absorption and Dispersion of Ultrasonic Waves* (Academic Press, New York, 1959).

23. D. Chandler, Accts. Chem. Res. 7, 246 (1974).

24. H. Eyring and R. P. Marchi, J. Chem. Educ. 40, 562 (1963).

25. D. A. McQuarrie, *Statistical Mechanics* (Harper and Row, New York, 1976), pp. 61-62.

26. T. L. Hill, *Intro. to Statistical Mechanics* (Addison-Wesley, Reading, Mass., 1960), pp. 36-37.

27. K. Arakawa and K. Kojima, Bull. Chem. Soc. Japan 48, 26 (1975).

28. W. G. Hoover and F. H. Ree, J. Chem. Phys. 49, 3609 (1968).

29. $\sigma^3 = 1.04/\rho_s$ is determined from Monte Carlo calculations on a system of hard spheres at the point of coexistence for the solid and fluid phases.

30. P. W. Anderson, J. Phys. Soc. Japan 9, 316 (1954).

31a. R. Kubo in Fluctuations, Relaxation, and Resonance in Magnetic Systems, ed. by D. ter Haar (Plenum, New York, 1962), p. 23 ff.

31b. Two limiting situations are distinguished by the relative magnitudes of Δ and τ_c. For $\Delta\tau_c \gg 1$, i.e. slow modulation, τ_c is large compared to $1/\Delta$ and the frequency intensity distribution mirrors the amplitude distribution of the modulation. Therefore, a Caussian distribution of frequency amplitude modulations yields a Gaussian lineshape. For $\Delta\tau_c \ll 1$, i.e. fast modulation, τ_c is small compared to $1/\Delta$ and the frequency intensity distribution approaches a Lorentzian in the limit $\Delta\tau_c \to 0$.

32. W. G. Rothschild, J. Chem. Phys. 65, 455 (1976); J. Chem. Phys. 65, 2958 (1976).

33. S. F. Fischer and A. Laubereau, Chem. Phys. Lett. 35, 6 (1975).

34. C. B. Harris, R. M. Shelby and P. A. Cornelius, Phys. Rev. Lett. 38, 1415 (1977).

35a. D. W. Oxtoby, J. Chem. Phys. 70, 2605 (1979).

35b. D. W. Oxtoby, D. Levesque and J. J. Weis, J. Chem. Phys. 68, 5528 (1978).

35c. D. J. Diestler and J. Manz, Mol. Phys. 33, 227 (1977).

35d. R. M. Lynden-Bell, Mol. Phys. 33, 907 (1977).

35e. D. J. Diestler, Chem. Phys. Lett. 39, 39 (1976).

35f. P. A. Madden and R. M. Lynden-Bell, Chem. Phys. Lett. 38, 163 (1976).

36a. S. Bratos and E. Merechal, Phys. Rev. A4, 1078 (1971).

36b. S. Bratos, J. Rios and Y. Guissani, J. Chem. Phys. 52, 439 (1970).

37. A. A. Orr, J. Paint. Technology 47, 45 (1975).

38. W. Gordy and S. C. Stanford, J. Chem. Phys. 9, 204 (1941).

39. J. A. Riddick and W. B. Bunger, Tech. in Chem., Vol. 2, *Organic Solvents* (John Wiley, New York, 1970).

40. J. Timmermans, *Physico-Chemical Constants of Pure Organic Compounds* (Elsevier Publishing Co., New York, 1950).

41. International Critical Tables 3, 45.

42. E. L. Heasell and J. Lamb, Proc. Phys. Soc. (London), B69, 869 (1956).

43. J. J. Markham, R. T. Beyer and R. B. Lindsay, Rev. Mod. Phys. 23, 353 (1951).

44. E. G. Richardson, *Ultrasonic Physics* (Elsevier Publishing Co., New York, 1962), p. 188-189.

45. A. Diamond, A. Fanelli and S. Petrucci, Inorg. Chem. 12, 611 (1973).

46. L. Werblan, J. Lesinski and L. Skubiszak, Roczniki Chemii, Ann. Soc. Chim. Polonorum 49, 221 (1975).

47. D. R. Dickson and P. Kruus, Canadian J. Chem. 49, 3107 (1971).

48. D. Sette, J. Chem. Phys. 19, 1337 (1951).

49. J. R. Pellam and J. K. Galt, J. Chem. Phys. 14, 608 (1946).

Table 1. Experimental dephasing times, calculated homogeneous linewidths, isotropic Raman linewidths and inhomogeneous broadening linewidths for the symmetric CH_3-stretching vibrations in the various liquids studied.

Table 2. Various liquid intermolecular attraction parameters.

Table 3. Parameters used to calculate the liquid's ultrasonic absorption constant.

Table 4. Parameters used to calculate the liquid's free volume.

Table 5. Calculated isothermal compressibilities, local number density distribution widths and the various parameters used in Equation 8.

Table 1

Molecule	$\omega(cm^{-1})$	average experimental T_2 (psec)	Calculated homogeneous $\Delta\omega(cm^{-1})$	Isotropic Raman Spontaneous $\Delta\omega(cm^{-1})$	Gaussian Inhomogeneous $\Delta\omega(cm^{-1})$
(1) 1,1,1-Trichloroethane	2938.5	2.6	4.1	4.3	0.9
(2) Methyl Iodide	2948	2.4	4.4	5.0	1.7
(3) Acetonitrile	2945	5.4	2.0	6.6	5.5
(4) Methyl Sulfide	2913.5	3.8	2.8	8.4	6.8
(5) Dimethyl Sulfoxide	2914.5	1.4	7.6	11.8	6.9
(6) Acetic Anhydride	2942.5	2.2	4.8	16.8	14.1
(7) Acetone	2925	3.0	3.5	16.5	14.6
(8) Methyl Formate	2961	2.2	4.8	17.5	14.8
(9) Pentane	2877	2.7	3.9	≈17	≈14.8
(10) Ethanol	2929	2.5	4.2	18.0	15.6
(11) Methanol	2836	2.4	4.4	18.8	16.3

/v

Table 2

	B.P./M.W.[a]	μ(D)[b]	H.B.P.(cm^{-1})[c]	g[d]
1,1,1-Trichloroethane	0.50	1.78	26[e]	1.315
Methyl Iodide	0.30	1.48	--	0.705
Acetonitrile	1.99	3.92	70[f]	1.005
Methyl Sulfide	0.60	1.50	--	0.883
Dimethyl Sulfoxide	2.41	3.96	155[f]	1.075
Acetic Anhydride	1.37	--	--	1.347
Acetone	0.97	2.88	75[f]	1.212
Methyl Formate	0.52	1.77	--	0.882
Pentane	0.50	0	0[g]	--
Ethanol	1.70	1.69	--	3.003
Methanol	1.96	1.70	187[h]	0.989

[a] Boiling point/Molecular weight

[b] Molecular dipole moment in Debyes.

[c] Hydrogen bonding parameter, in wavenumbers, cm^{-1}, reference 37.

[d] Kirkwood dipole correlation factor. Reference 19. Calculated using eqn.(3.4) on p. 108. Parameters used in that expression were obtained from reference 39.

[e] Reference 37. Data for 1,1,2-Trichloroethane.

[f] Reference 37.

[g] Reference 37. Data for n-heptane.

[h] Reference 38. Data for CH_3OD.

/v

Table 3

	c (cm/sec)[a]	η(cp)[b]	α[c]	α/α_{class}[d]
1,1,1-Trichloroethane	102,000[e]	0.832	436[m]	28.5
Methyl Iodide	84,000[f,g]	0.460	315[f,m,n,o]	34.9
Acetonitrile	128,000[f]	0.360	72[f,p]	12.5
Methyl Sulfide	100,000[h]	0.293	59[m]	6.7
Dimethyl Sulfoxide	148,900[i]	1.996	36[i,q]	2.6
Acetic Anhydride	115,000[j]	0.852	58[m]	4.6
Acetone	117,000[f]	0.327	30-70[f,m,n]	4-10
Methyl Formate	126,000[k]	0.347	49[m]	11.1
Pentane	108,500[l]	0.233	72[r,s,t,u]	7.1
Ethanol	115,000[f]	1.180	54[n]	2.1
Methanol	112,000[f]	0.597	32[m,n]	2.3

a) Sound speed

b) Viscosity in centipoise.

c) Observed ultrasonic absorption coefficient. $\alpha = (\alpha/f^2)_{observed}$ in $sec^2/cm \times 10^{-17}$.

d) Ultrasonic absorption constant. $\alpha_{class} = (\alpha/f^2)_{classical} = 8\pi^2\eta/3\rho c^3$. Reference 21,22.

e) Reference 48. Value for 1,1-Dichloroethane

f) Reference 44.

g) Reference 49.

h) Reference 44. Value for ethyl ether.

i) Reference 47.

j) Reference 44. Value similar to acetates.

k) Reference 44. Value for ethyl formate.

l) Reference 49. Value for hexane.

m) Reference 42.

n) Reference 43.

o) Reference 21.

p) Reference 45.

q) Reference 46.

r) Reference 42. Value for hexane.

s) Reference 43. Value for hexane.

t) Reference 21. Value for hexane.

u) Reference 44. Value for hexane.

/v

Table 4

	ρ_l (25°) (gm/cm^3) [a]	ρ_s (M.P.) (gm/cm^3) [b]	% free volume
1,1,1-Trichloroethane	1.3293	1.4204 [c]	5.7
Methyl Iodide	2.2649	2.5211 [c]	10.2
Acetonitrile	0.7766	0.8512 [d]	8.7
Methyl Sulfide	0.8423	0.9796 [c]	14.0
Dimethyl Sulfoxide	1.0958	1.1022 [e]	0.6
Acetic Anhydride	1.0751	1.1937 [c]	10.0
Acetone	0.7844	0.9157 [d]	16.2
Methyl Formate	0.9669	1.1447 [c]	14.9
Pentane	0.6214	0.7683 [d]	18.5
Ethanol	0.7850	0.9014 [f]	12.4
Methanol	0.7866	0.9673 [g]	18.2

a) Liquid densities at 25°C from reference 39.

b) Solid densities at the melting point.

c) Reference 40. Value extrapolated from 0°C.

d) Reference 40.

e) Reference 39. Value calculated using formula.

f) Reference 40. Value calculated using formula.

g) Reference 41.

Table 5

	y^a	K_o^{-1} (J/cm^3)^b	$\frac{\Delta H_{vap}}{V}$ (J/cm^3)^c	$\frac{RT}{V}$ (J/cm^3)^d	K_T^{-1} (J/cm^3)^e	$\sigma_\rho \propto \rho\sqrt{K_T}^f$
1,1,1-Trichloroethane	0.510	1740	322	25	1146	294
Methyl Iodide	0.489	2273	439	40	1474	416
Acetonitrile	0.497	2906	629	47	1742	453
Methyl Sulfide	0.468	1575	375	34	892	454
Dimethyl Sulfoxide	0.541	3408	742	35	1994	314
Acetic Anhydride	0.490	1518	482	26	607	427
Acetone	0.467	1543	417	33	777	484
Methyl Formate	0.460	1730	455	40	900	537
Pentane	0.440	770	228	21	357	456

[a] Liquid packing fraction. Calculated using Equations 8 and 9.

[b] Calculated using Equation 7.

[c] Heats of vaporization per cm^3 at 25°C from Reference 39.

[d] Thermal energy per cm^3 at 25°C.

[e] Calculated using Equation 6.

[f] Calculated using the important terms in Equation 5.

Figure 1. Experimental setup for stimulated Stokes excitation and selective, collinear coherent Stokes probe scattering. Excitation Stokes and coherent probe Stokes signals are spatially separated and simultaneously detected on the target of a two-dimensional OMA.

Figure 2. Experimental data for the symmetric CH_3-stretching vibration in methanol and ethanol. Coherently scattered Stokes signal as a function of probe pulse delay in (a) methanol and (c) ethanol. Isotropic Raman lineshapes and homogeneous Lorentzian lineshapes calculated from the measured dephasing times in (b) methanol and (d) ethanol.

Figure 3. Experimental data for the symmetric CH_3-stretching vibration in acetone and methyl sulfide. Coherently scattered Stokes signal as a function of probe pulse delay in (a) acetone and (c) methyl sulfide. Isotropic Raman lineshapes and homogeneous Lorentzian lineshapes calculated from the measured dephasing times in (b) acetone and (d) methyl sulfide.

Figure 4. Experimental data for the symmetric CH_3-stretching vibration in trichloroethane and acetonitrile. Coherently scattered Stokes signal as a function of probe pulse delay in (a) trichloroethane and (c) acetonitrile. Isotropic Raman lineshapes and homogeneous Lorentzian lineshapes calculated from the measured dephasing times in (b) trichloroethane and (d) acetonitrile.

Figure 5. Graph of the inhomogeneous broadening linewidth versus the liquid's intermolecular attraction parameter as defined by (B.P./ M.W.).

Figure 6. Graph of the inhomogeneous broadening linewidth versus the liquid's hydrogen bonding parameter. (cf. Ref. 37,38)

Figure 7. Graph of the inhomogeneous broadening linewidth versus the molecular dipole moment.

Figure 8. Graph of the inhomogeneous broadening linewidth versus the liquid's dipole correlation factor. (cf. Ref. 19,20)

Figure 9. Graph of the inhomogeneous broadening linewidth versus the liquid's ultrasonic absorption constant. (cf. Ref. 21,22)

Figure 10. Graph of the inhomogeneous broadening linewidth versus the liquid's free volume percentage. (See Table 4 for details)

Figure 11. Graph of the inhomogeneous broadening linewidth versus the liquid's local number density distribution width as calculated from Equations 5-9.

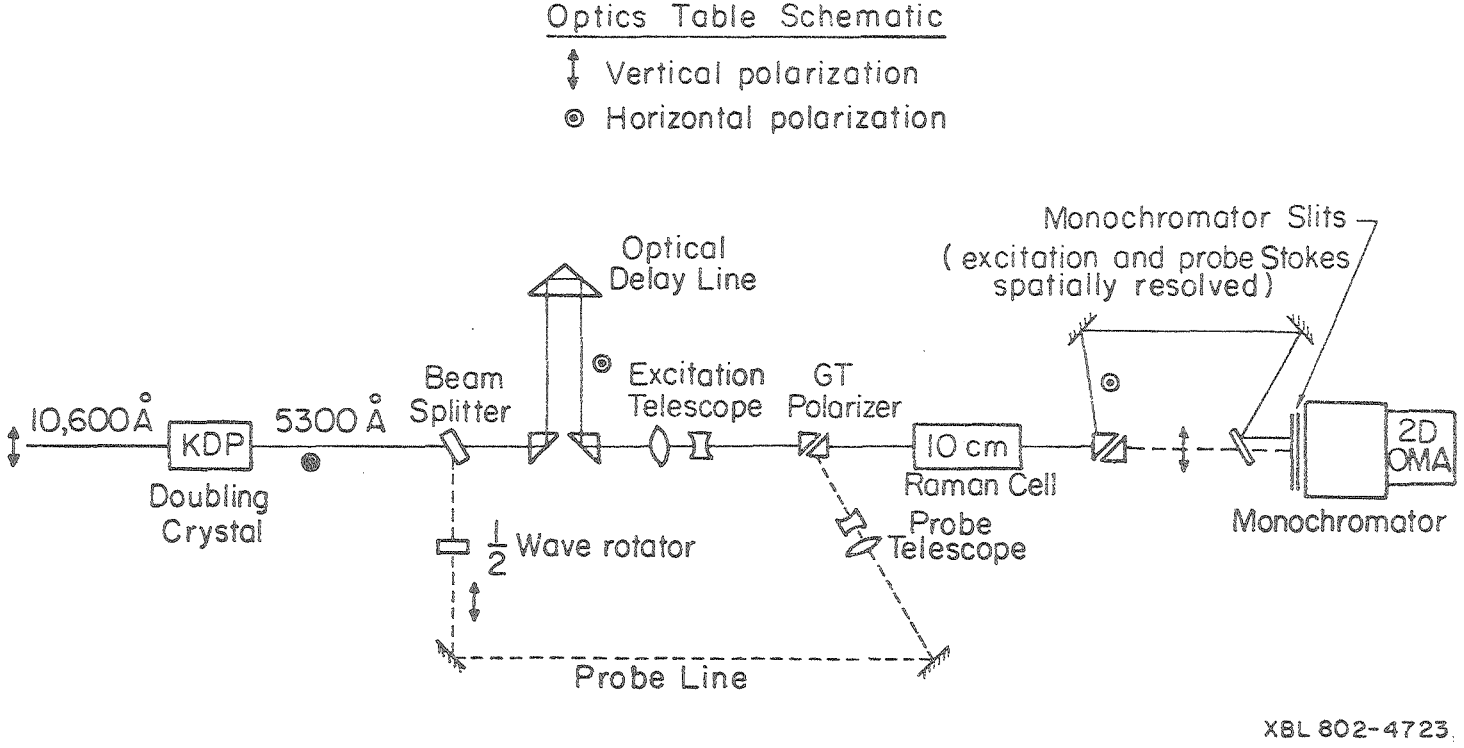
Optics Table Schematic
Vertical polarization
Horizontal polarization
Monochromator Slits
(excitation and probe Stokes
spatially resolved)
Optical
Delay Line
Beam
Splitter
Excitation
Telescope
GT
Polarizer
10,600 Å
KDP
Doubling
Crystal
5300 Å
10 cm
Raman Cell
2D
OMA
Monochromator
Probe
Telescope
1/2 Wave rotator
Probe Line
XBL 802-4723

Figure 1

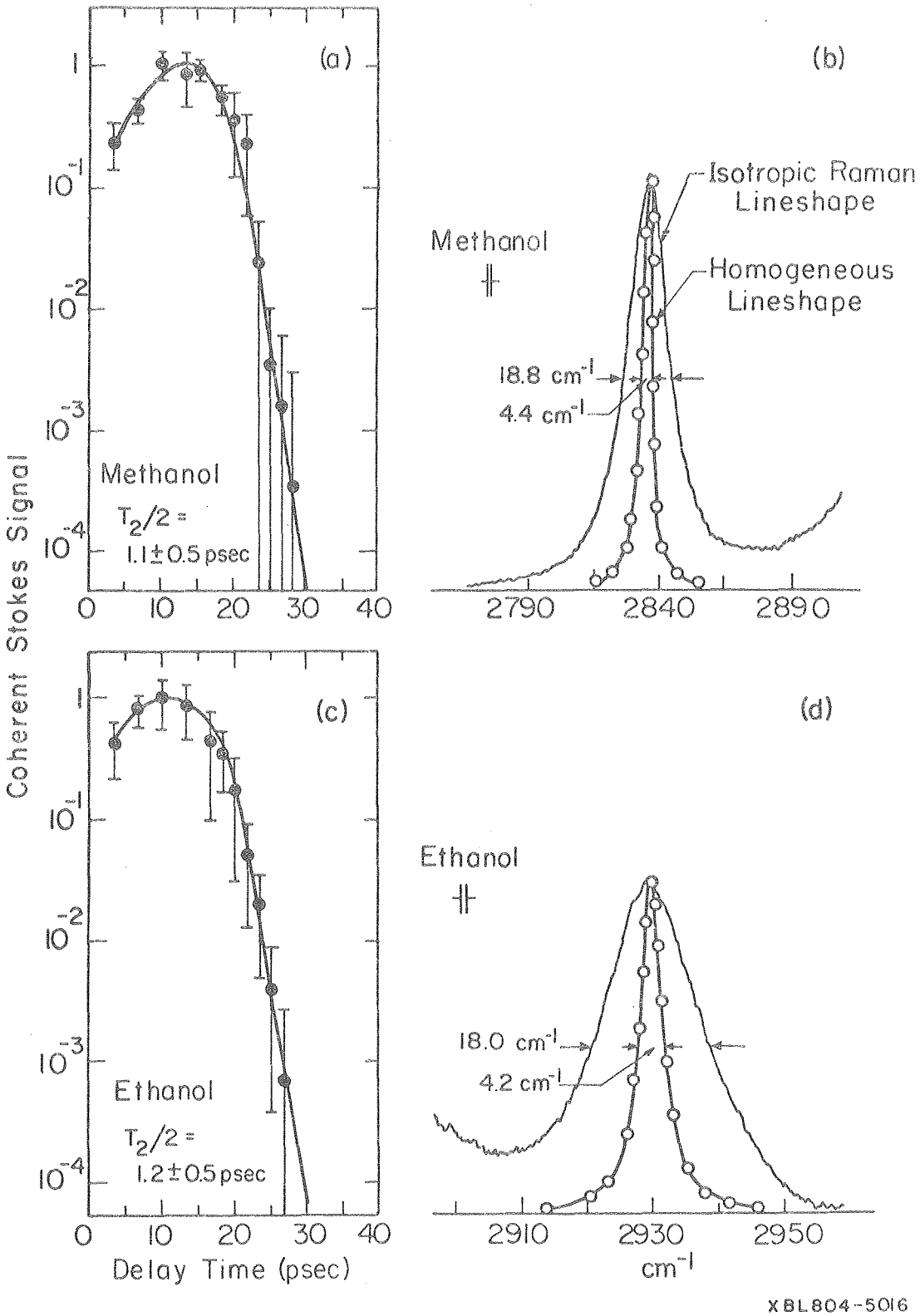
(a)
(b)
(c)
(d)
Coherent Stokes Signal
Methanol
$T_2/2$ = 1.1±0.5 psec
Ethanol
$T_2/2$ = 1.2±0.5 psec
Isotropic Raman Lineshape
Homogeneous Lineshape
18.8 cm⁻¹
4.4 cm⁻¹
18.0 cm⁻¹
4.2 cm⁻¹
Delay Time (psec)
cm⁻¹
XBL804-5016

Figure 2

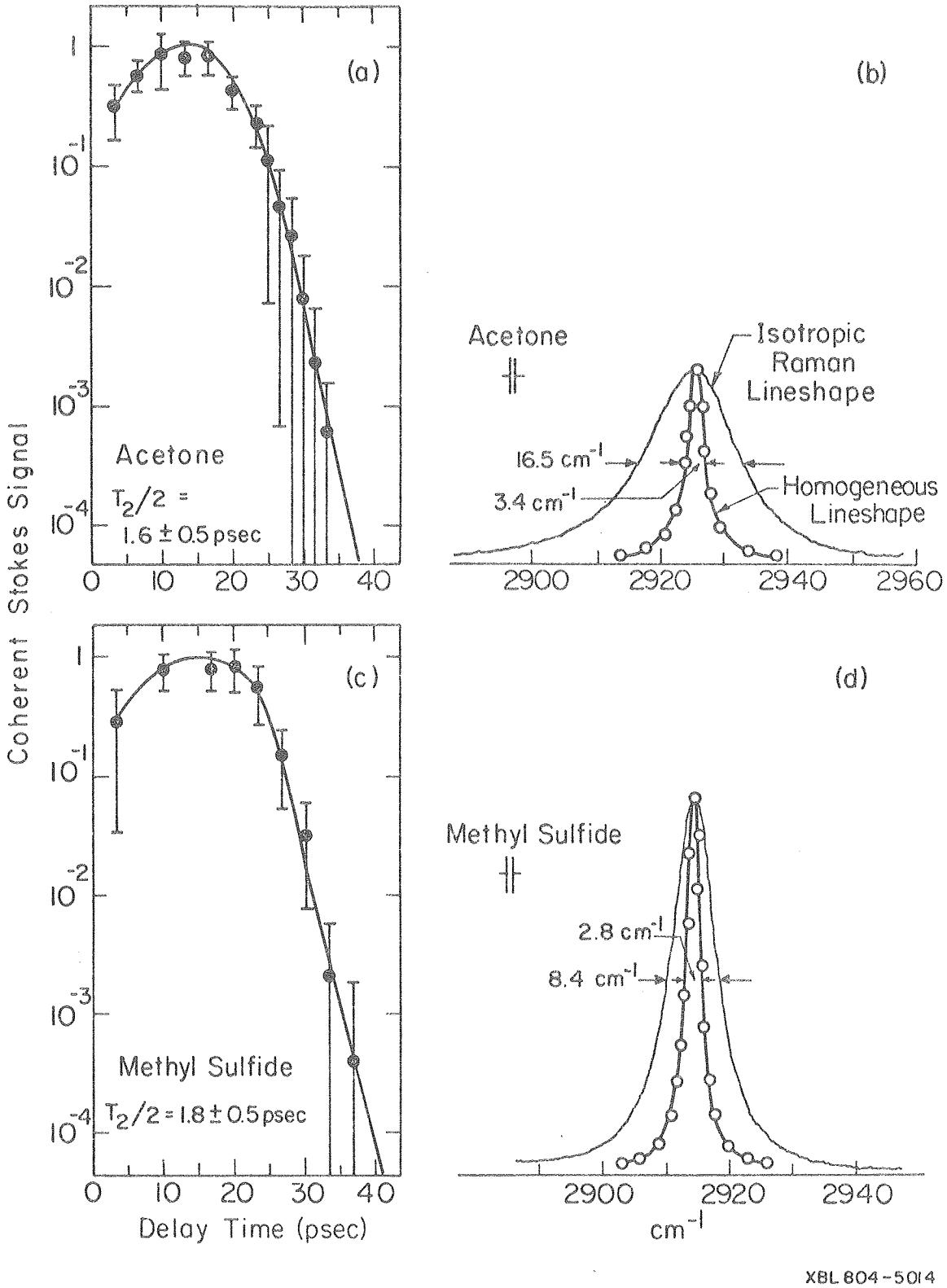
(a)
Acetone
$T_2/2$ =
1.6 ± 0.5 psec
Coherent Stokes Signal
Delay Time (psec)
(b)
Acetone
Isotropic
Raman
Lineshape
16.5 cm⁻¹
3.4 cm⁻¹
Homogeneous
Lineshape
2900
2920
2940
2960
(c)
Methyl Sulfide
$T_2/2$ = 1.8 ± 0.5 psec
(d)
Methyl Sulfide
2.8 cm⁻¹
8.4 cm⁻¹
2900
2920
2940
cm⁻¹
XBL 804-5014

Figure 3

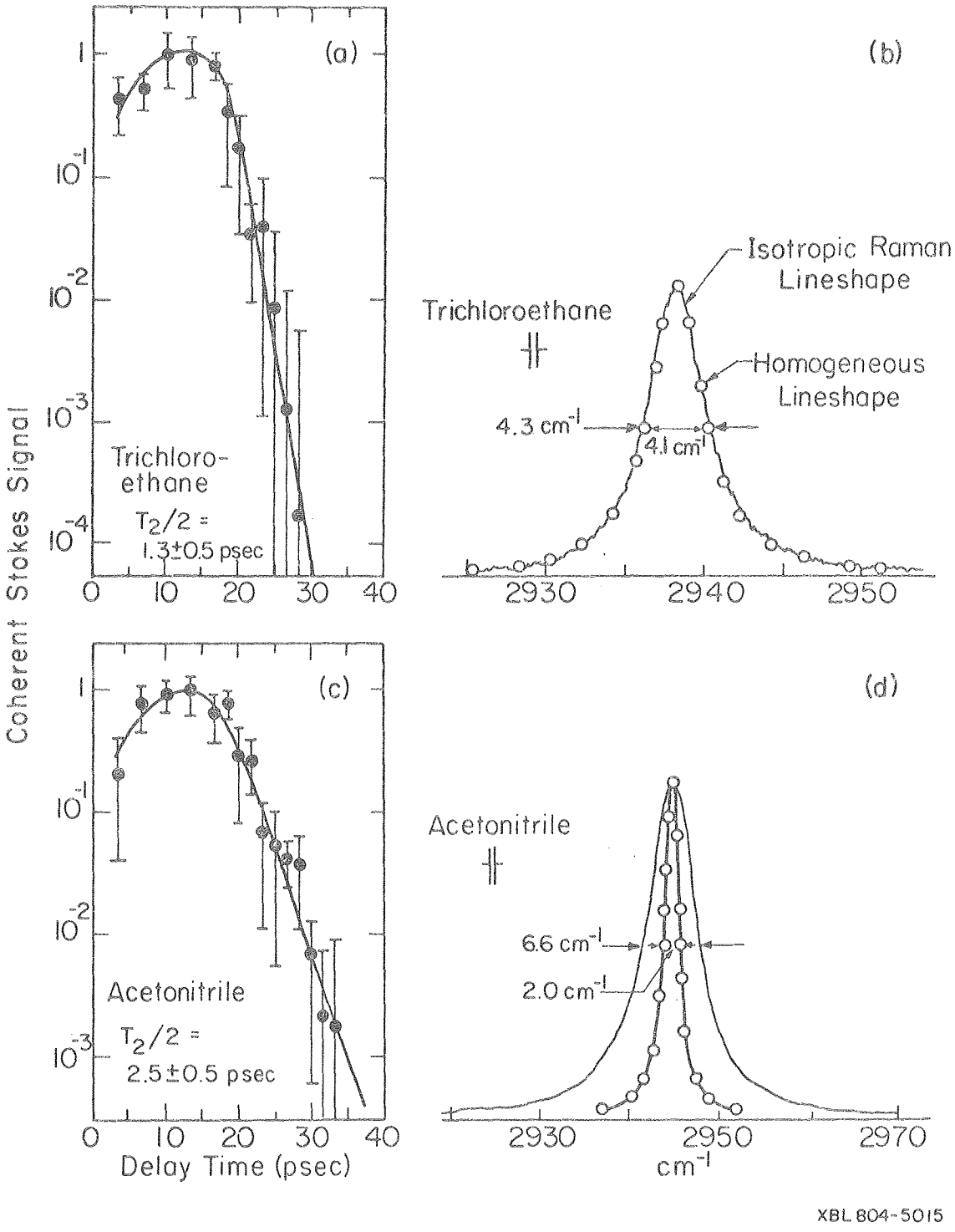
(a)
(b)
(c)
(d)
Coherent Stokes Signal
Trichloro-
ethane
$T_2/2$ =
1.3±0.5 psec
Isotropic Raman
Lineshape
Trichloroethane
Homogeneous
Lineshape
4.3 cm^{-1}
4.1 cm^{-1}
Acetonitrile
$T_2/2$ =
2.5±0.5 psec
Acetonitrile
6.6 cm^{-1}
2.0 cm^{-1}
Delay Time (psec)
cm^{-1}
XBL 804-5015

Figure 4

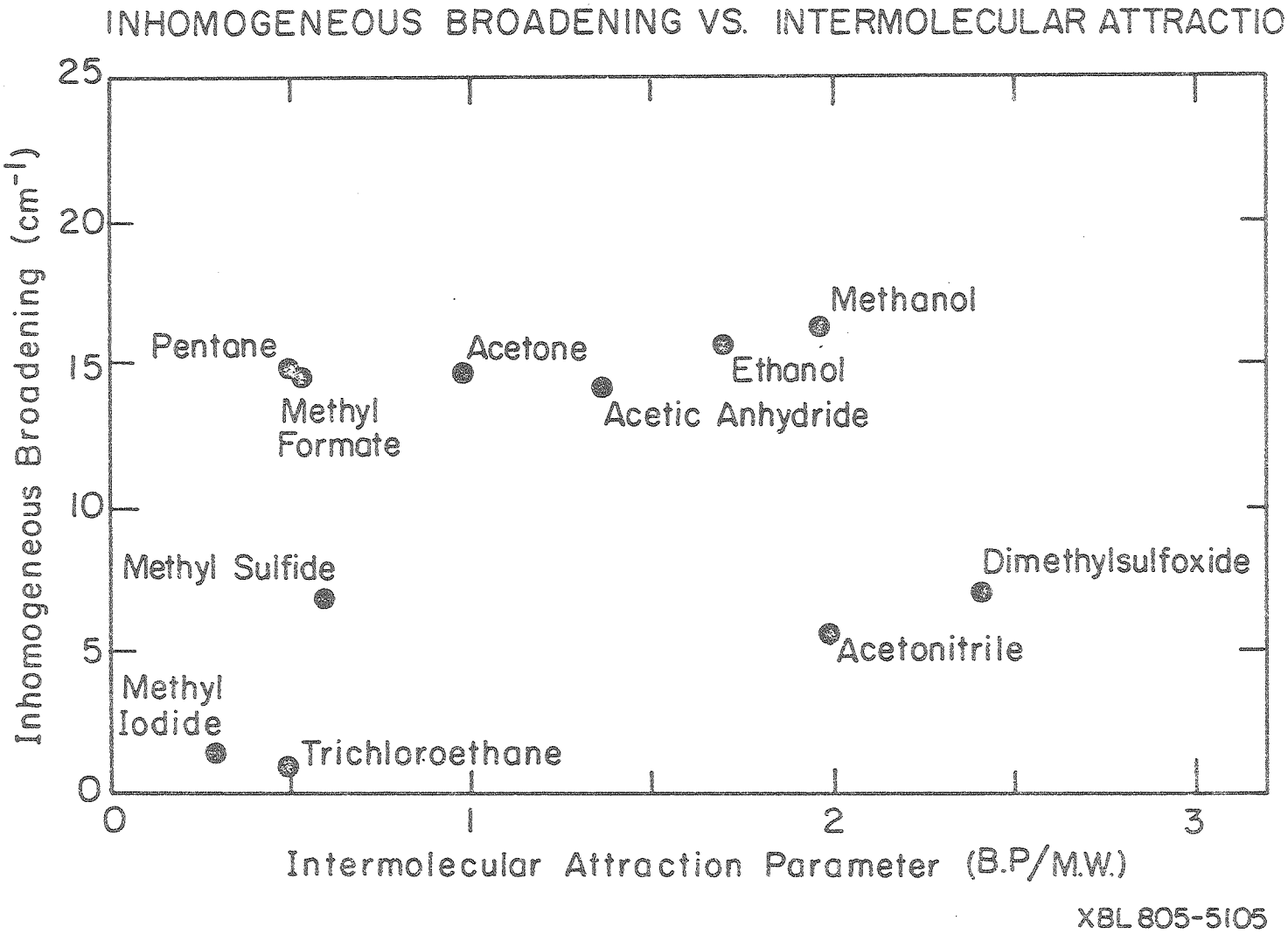
INHOMOGENEOUS BROADENING VS. INTERMOLECULAR ATTRACTION
Inhomogeneous Broadening (cm⁻¹)
25
20
15
10
5
0
0
1
2
3
Intermolecular Attraction Parameter (B.P/M.W.)
Pentane
Methyl Formate
Acetone
Methanol
Ethanol
Acetic Anhydride
Methyl Sulfide
Dimethylsulfoxide
Acetonitrile
Methyl Iodide
Trichloroethane
XBL 805-5105

Figure 5

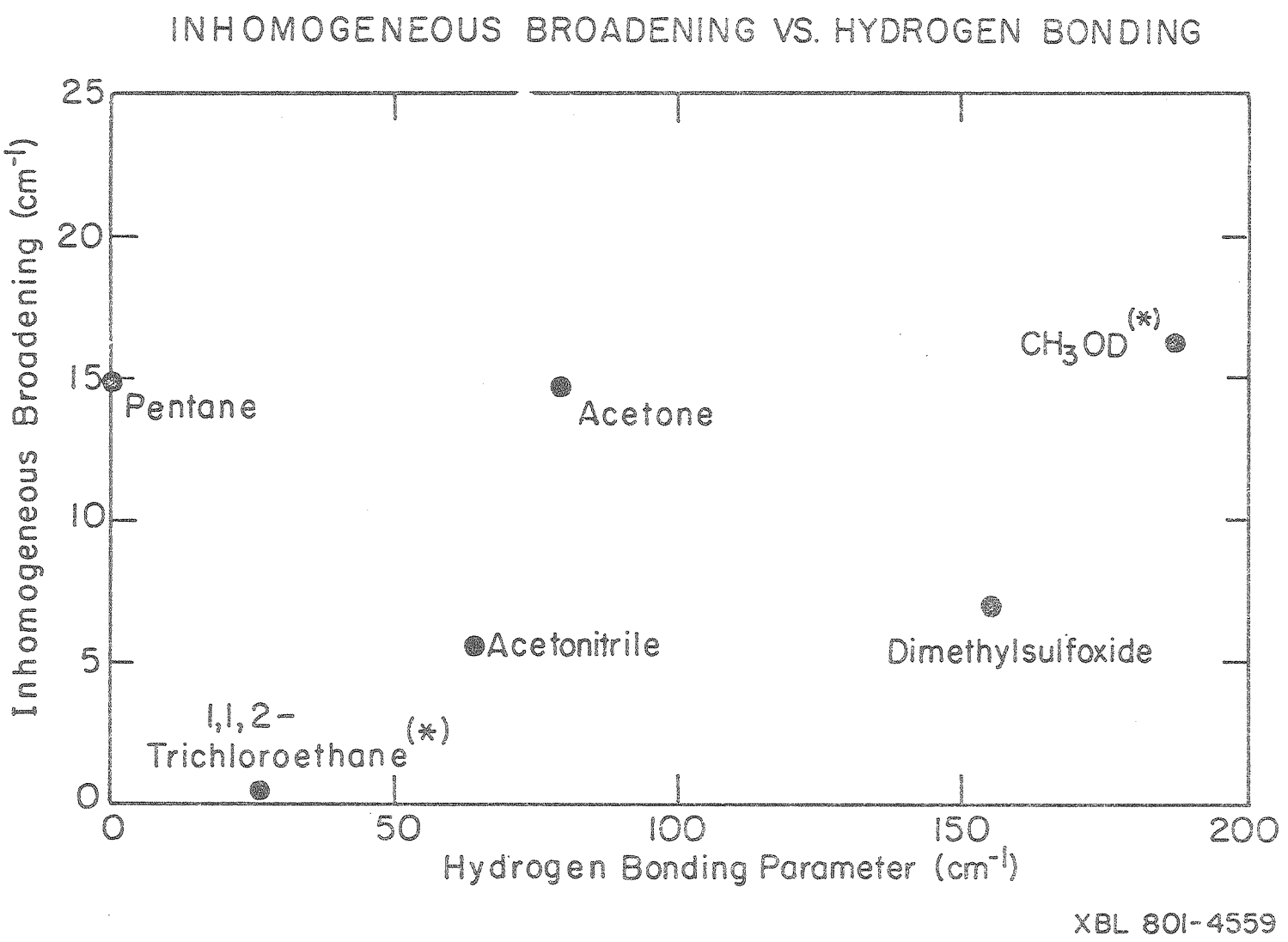
INHOMOGENEOUS BROADENING VS. HYDROGEN BONDING
Inhomogeneous Broadening (cm⁻¹)
25
20
15
10
5
0
Pentane
Acetone
CH3OD (*)
Acetonitrile
Dimethylsulfoxide
1,1,2-
Trichloroethane (*)
0
50
100
150
200
Hydrogen Bonding Parameter (cm⁻¹)
XBL 801-4559

Figure 6

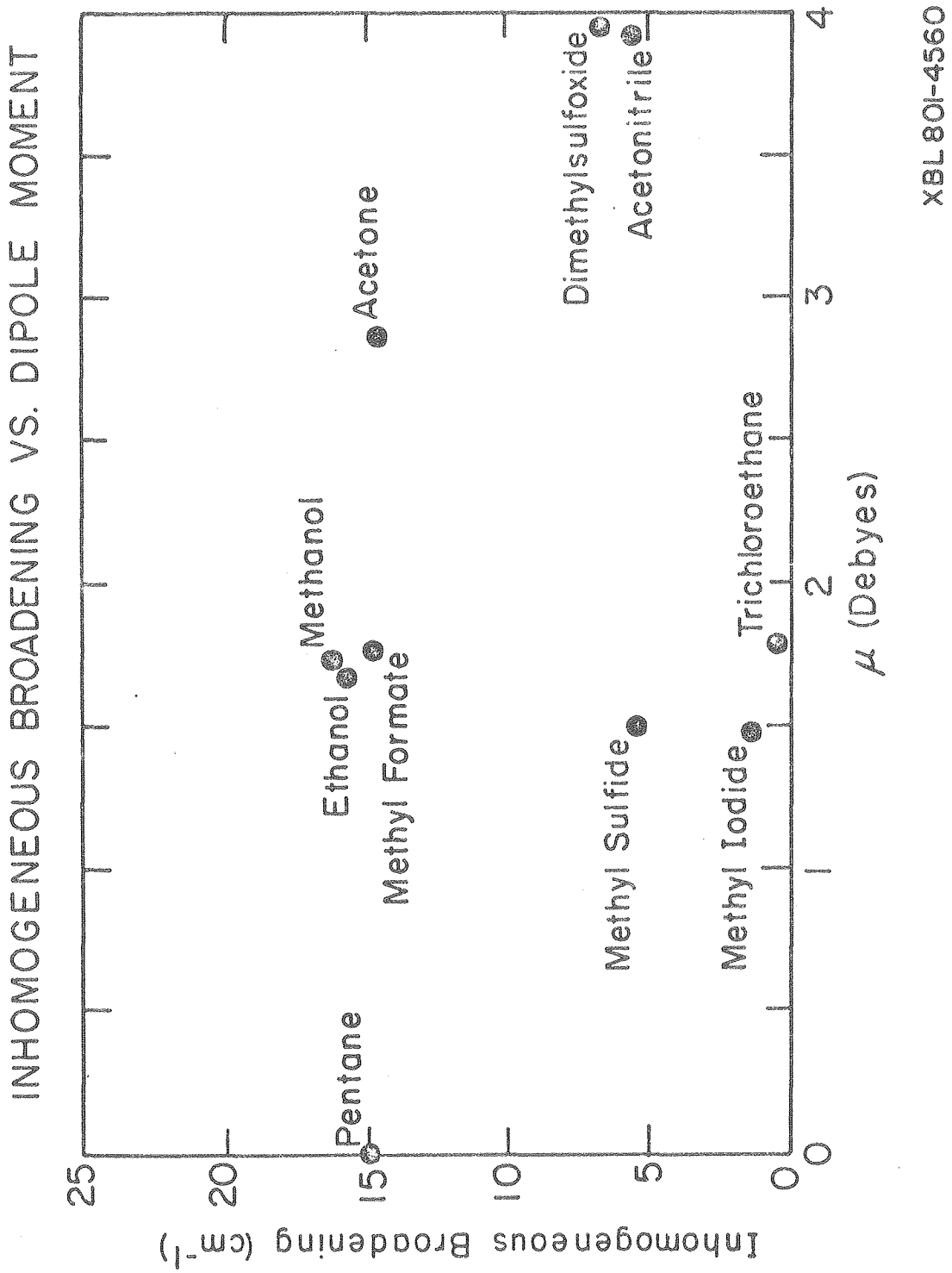
INHOMOGENEOUS BROADENING VS. DIPOLE MOMENT
Inhomogeneous Broadening (cm⁻¹)
μ (Debyes)
0
5
10
15
20
25
0
1
2
3
4
Pentane
Ethanol
Methanol
Methyl Formate
Acetone
Methyl Sulfide
Methyl Iodide
Trichloroethane
Dimethylsulfoxide
Acetonitrile
XBL801-4560

Figure 7

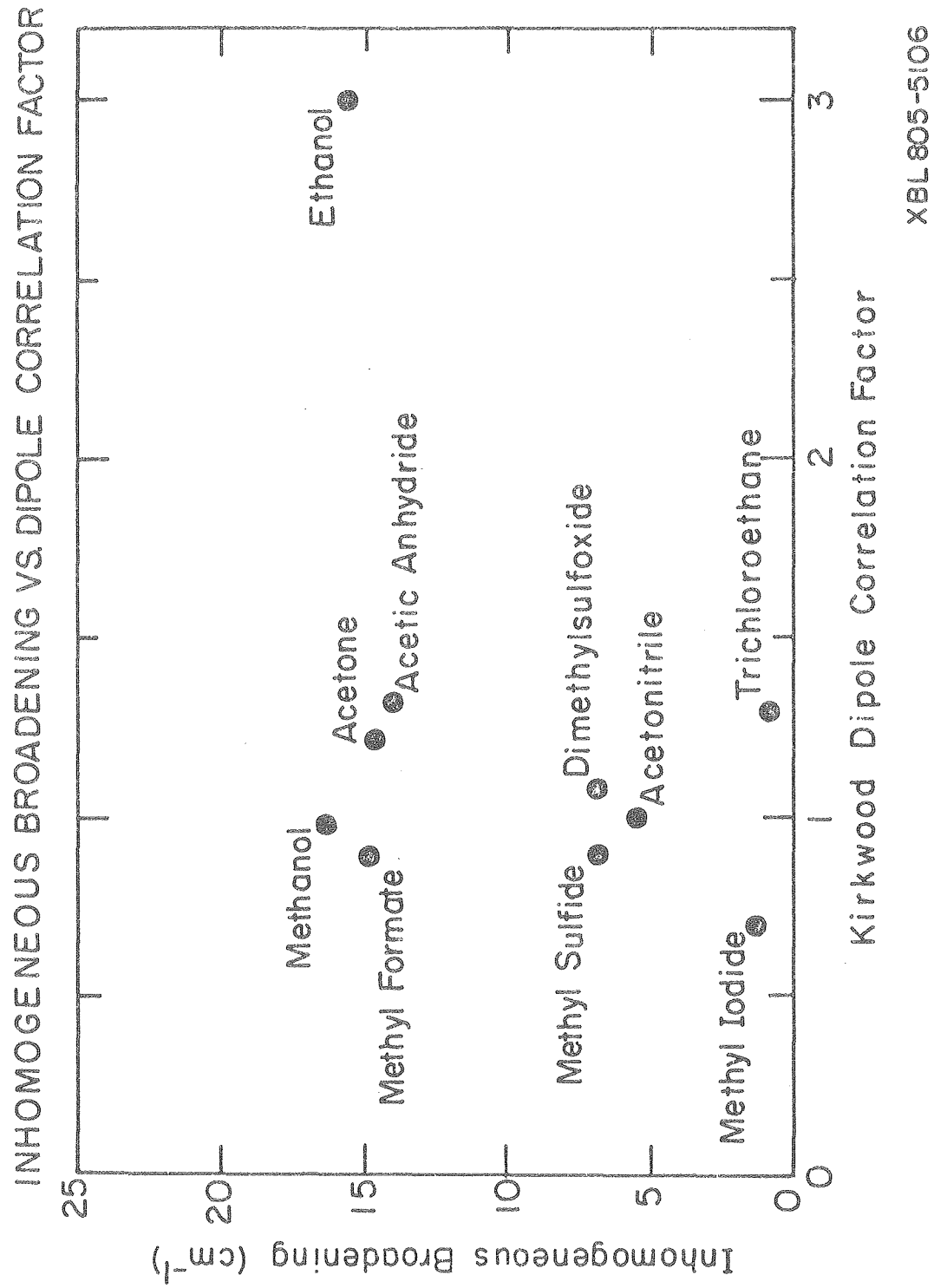
INHOMOGENEOUS BROADENING VS. DIPOLE CORRELATION FACTOR
Inhomogeneous Broadening (cm⁻¹)
Kirkwood Dipole Correlation Factor
0
5
10
15
20
25
0
1
2
3
Ethanol
Methanol
Acetone
Acetic Anhydride
Methyl Formate
Methyl Sulfide
Dimethylsulfoxide
Acetonitrile
Trichloroethane
Methyl Iodide
XBL805-5106

Figure 8

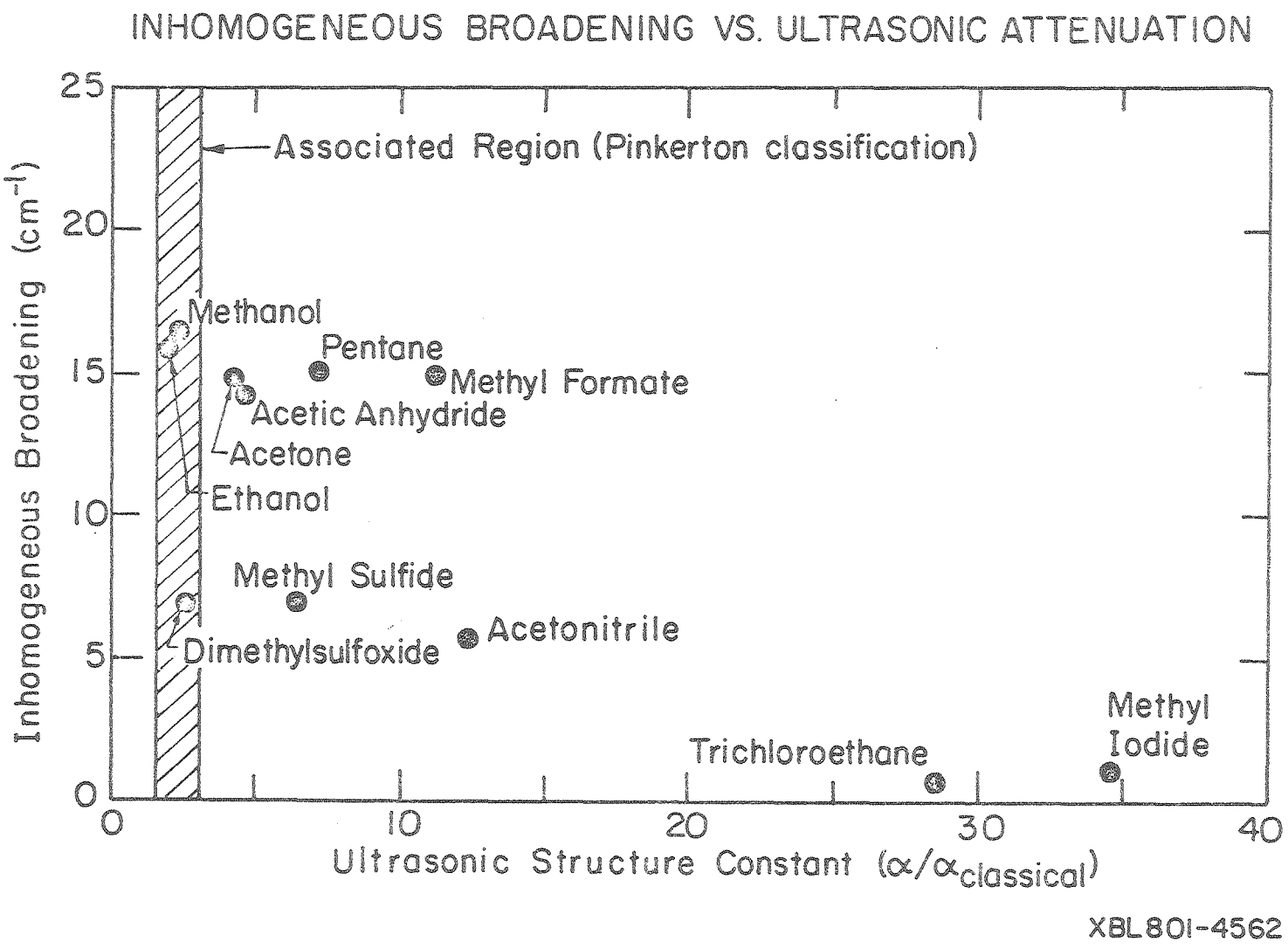
INHOMOGENEOUS BROADENING VS. ULTRASONIC ATTENUATION
Inhomogeneous Broadening (cm^{-1})
Ultrasonic Structure Constant ($\alpha/\alpha_{classical}$)
Associated Region (Pinkerton classification)
Methanol
Pentane
Methyl Formate
Acetic Anhydride
Acetone
Ethanol
Methyl Sulfide
Acetonitrile
Dimethylsulfoxide
Trichloroethane
Methyl Iodide
0
5
10
15
20
25
0
10
20
30
40
XBL801-4562

Figure 9

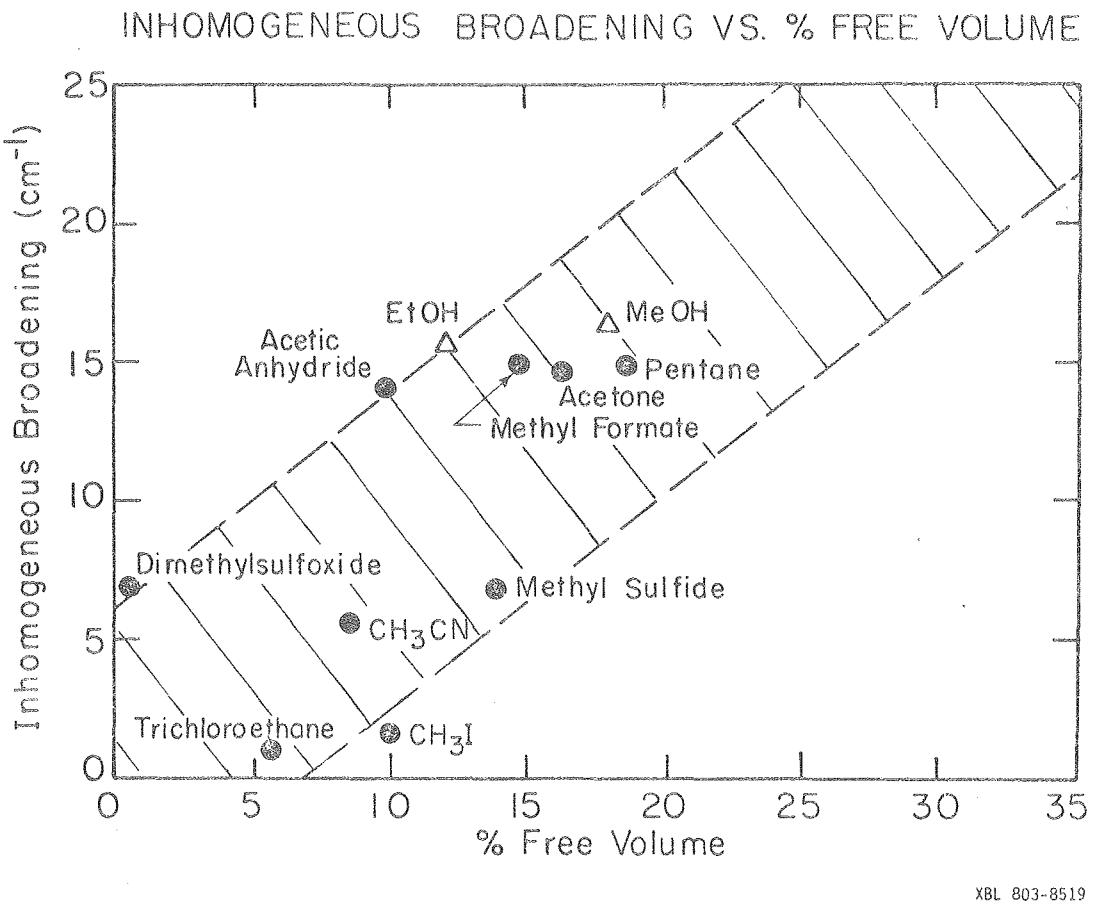
INHOMOGENEOUS BROADENING VS. % FREE VOLUME
Inhomogeneous Broadening (cm^{-1})
% Free Volume
0
5
10
15
20
25
30
35
EtOH
MeOH
Acetic Anhydride
Pentane
Acetone
Methyl Formate
Dimethylsulfoxide
Methyl Sulfide
CH_3CN
Trichloroethane
CH_3I
XBL 803-8519

Figure 10

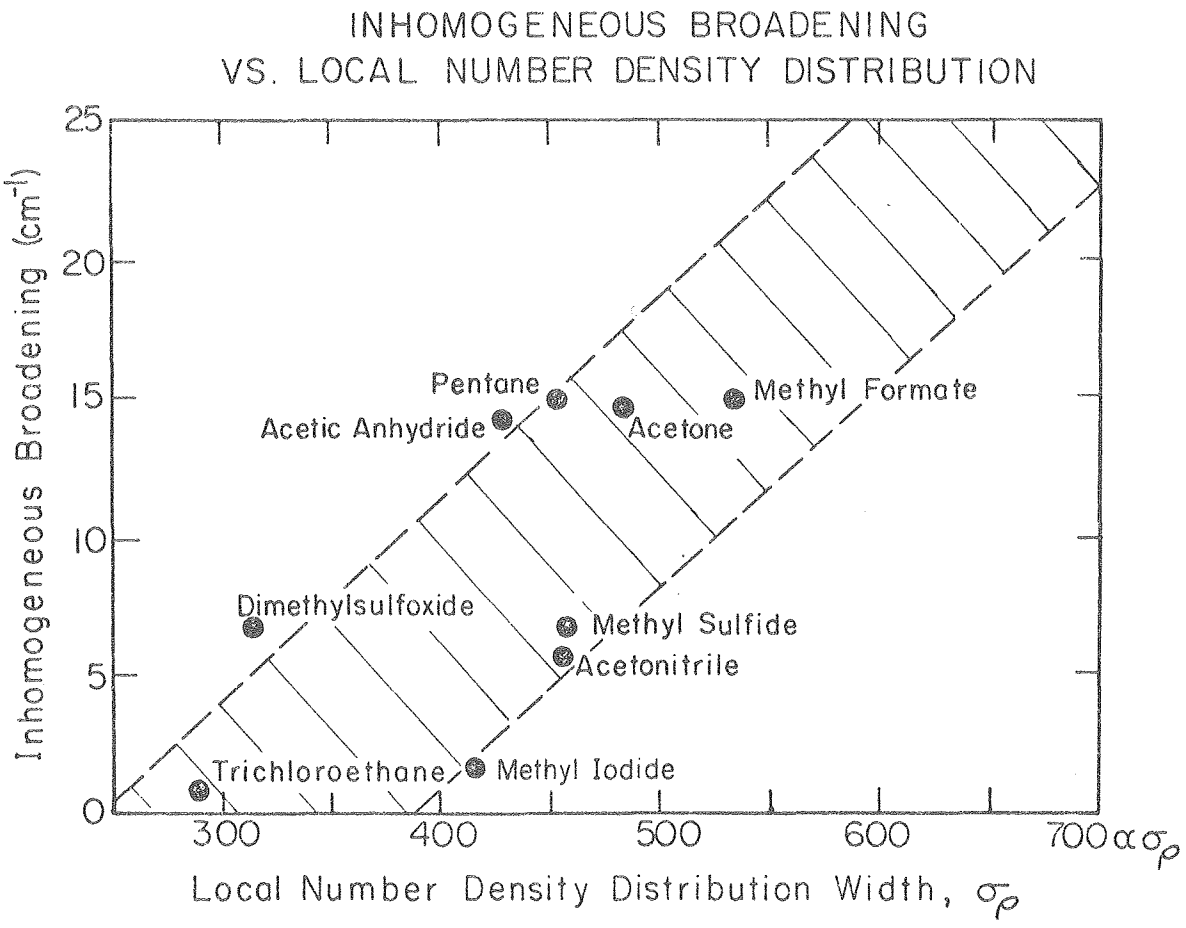
INHOMOGENEOUS BROADENING
VS. LOCAL NUMBER DENSITY DISTRIBUTION
Inhomogeneous Broadening (cm⁻¹)
25
20
15
10
5
0
Pentane
Methyl Formate
Acetic Anhydride
Acetone
Dimethylsulfoxide
Methyl Sulfide
Acetonitrile
Trichloroethane
Methyl Iodide
300
400
500
600
700 α σρ
Local Number Density Distribution Width, σρ
XBL 803-8518

Figure 11